Check for updates

Geophysical Research Letters

RESEARCH LETTER
10.1029/2022GL101175

Key Points:

- We observe short and long-term variations in the thumping cycle recorded by two geophones deployed between 2015 and 2021
- On hourly to daily time scales, the time to initiate thumping correlates with the wind speed
- On monthly to yearly time scales, cycle variations reflect changes in heating rate that vary by a factor of about 2

Supporting Information:

Supporting Information may be found in the online version of this article.

Correspondence to:

C.-N. Liu,
cheng-nan.liu@utah.edu

Citation:

Liu, C.-N., Lin, F.-C., Manga, M., Farrell, J., Wu, S.-M., Reed, M. H., et al. (2023). Thumping cycle variations of Doublet Pool in Yellowstone National Park, USA. *Geophysical Research Letters*, *50*, e2022GL101175. https://doi.org/10.1029/2022GL101175

Received 8 SEP 2022
Accepted 31 JAN 2023

Author Contributions:

Conceptualization: Fan-Chi Lin, Michael Manga, Anna Barth
Data curation: Jamie Farrell, Jefferson Hungerford, Erin White
Formal analysis: Cheng-Nan Liu, Michael Manga
Funding acquisition: Fan-Chi Lin, Michael Manga, Jamie Farrell
Investigation: Cheng-Nan Liu, Michael Manga, Mara H. Reed, Anna Barth
Methodology: Fan-Chi Lin, Michael Manga, Sin-Mei Wu, Anna Barth
Project Administration: Fan-Chi Lin, Michael Manga, Jamie Farrell

© 2023. The Authors.
This is an open access article under the terms of the Creative Commons Attribution-NonCommercial-NoDerivs License, which permits use and distribution in any medium, provided the original work is properly cited, the use is non-commercial and no modifications or adaptations are made.

Thumping Cycle Variations of Doublet Pool in Yellowstone National Park, USA

Cheng-Nan Liu[1], Fan-Chi Lin[1], Michael Manga[2], Jamie Farrell[1], Sin-Mei Wu[1,3], Mara H. Reed[2], Anna Barth[2], Jefferson Hungerford[4], and Erin White[4]

[1]Department of Geology and Geophysics, University of Utah, Salt Lake City, UT, USA, [2]Department of Earth and Planetary Science, University of California, Berkeley, CA, USA, [3]Swiss Seismological Service, ETH Zurich, Zurich, Switzerland, [4]Yellowstone Center for Resources, Yellowstone National Park, WY, USA

Abstract Doublet Pool is an active hydrothermal feature in Yellowstone National Park, USA. Approximately every half hour, it thumps for about 10 min due to bubbles collapsing at the base of the pool. To understand its thermodynamics and sensitivity to external factors, we performed a recurring multiple-year passive seismic experiment. By linking recorded hydrothermal tremor with active thumping, we determine the onset and end of thumping, and the duration of silence between each thumping cycle. The silence interval decreased from around 30 min before November 2016 to around 13 min in September 2018. This change followed unusual thermal activity on the surrounding Geyser Hill. On a shorter time scale, wind-driven evaporative cooling can lengthen the pre-thumping silence interval. Based on energy conservation, we determine the heating rate and heat needed to initiate thumping to be 3–7 MW and ~6 GJ, respectively.

Plain Language Summary Doublet Pool is a hot spring in Yellowstone that has thumping cycles in which bubbles collapse underwater, producing vibrations that people can hear and feel. We placed two seismometers next to Doublet Pool to time its thumping cycles and analyze how they change over time. Strong winds lengthen the thumping interval by removing energy through the pool's surface. Over time scales of months to years, the duration of thumping cycles is controlled by changes in heating and pressurization from the hydrothermal system beneath Doublet Pool.

1. Introduction

The active Yellowstone hydrothermal system results from shallow groundwater interacting with heat from a deeper magmatic system (Smith & Siegel, 2000). Variations in heating rate, conduit geometry, and water influx control the exact surface manifestation of each hydrothermal feature (e.g., Namiki et al., 2016; Rinehart, 1980; Toramaru & Maeda, 2013). An eruptive geyser is composed of a long narrow subsurface conduit with constrictions that inhibit effective fluid convection, keep the hydrostatic pressure high, and suppress the liquid-to-vapor phase transition. With continued heat accumulation, the system eventually reaches a critical condition where a perturbation in pressure initiates a phase transition between liquid and vapor, and the resulting volume expansion will vigorously eject a liquid-vapor mixture into the air (White, 1967). A hot spring, in contrast, is a steady-state system where both heat and water influx and outflux remain balanced. At least one hot spring in New Zealand (Iodine Pool; Legaz et al., 2009) and several features in Yellowstone, however, mysteriously "thump" either periodically or episodically suggesting their heat input and output are not completely balanced and thus that they share some similarities with geysers. Doublet Pool, a hot spring composed of a main and an auxiliary pool connected by a narrow channel at the surface, in the Upper Geyser Basin (Figure 1), is famous for its persistent, approximately periodic thumping cycle (Bryan, 2008). During active thumping, the water level in the main pool vibrates visibly, ground shaking can be felt, and thumping can be heard on a quiet day near the pool. While periodic thumping resembles a geyser's eruption pattern, the thumping at Doublet Pool never evolves into an active eruption.

Many previous geophysical studies, including seismic investigations aimed at understanding the eruption dynamics of geysers, have recorded hydrothermal tremor connected to the liquid/vapor phase transition processes (Kedar et al., 1998, 1996; Wu et al., 2017). The spatiotemporal distribution of the tremor sources has been used to illuminate the subsurface conduit system and infer the physical state of the geyser system during each stage of the eruption cycle (Eibl et al., 2021; Vandemeulebrouck et al., 2013; Wu et al., 2019, 2021). Simultaneous seismic and in

19448007, 2023, 4, Downloaded from https://agupubs.onlinelibrary.wiley.com/doi/10.1029/2022GL101175 by University Of Utah, Wiley Online Library on [15/02/2023]. See the Terms and Conditions (https://onlinelibrary.wiley.com/terms-and-conditions) on Wiley Online Library for rules of use; OA articles are governed by the applicable Creative Commons License

Software: Sin-Mei Wu
Supervision: Fan-Chi Lin, Michael Manga
Validation: Fan-Chi Lin, Michael Manga, Mara H. Reed, Anna Barth
Writing – original draft: Cheng-Nan Liu
Writing – review & editing: Fan-Chi Lin, Michael Manga, Jamie Farrell, Sin-Mei Wu, Mara H. Reed, Anna Barth

situ pressure recordings confirmed bubble collapse in a shallow conduit during the preparation stage of a geyser eruption as one of the major sources of hydrothermal tremor (Kedar et al., 1998), although other tremor source mechanisms such as conduit resonance and bubble nucleation have also been proposed (Munoz-Saez, Namiki, et al., 2015; Munoz-Saez, Manga et al., 2015; Nayak et al., 2020; Rudolph et al., 2018; Vandemeulebrouck et al., 2014; Wu et al., 2019). These observations and proposed mechanisms also share some similarities to volcanic banded tremor (Cannata et al., 2010; Fujita, 2008). By estimating the water volume and temperature change of water ejected through eruptions, thermodynamic parameters such as the heat output rate of geysers can be estimated (N. Fournier et al., 2009) but it is unclear how these insights apply to thumping hot springs.

Investigating thumping, presumably a more energetic manifestation of hydrothermal tremor, of a hot spring such as Doublet Pool offers an opportunity to advance our fundamental knowledge of unsteady hydrothermal systems. Unlike eruptive geysers, in situ measurements (e.g., pressure, temperature, acoustic, and video) can be conducted without interruptions by eruptions. Our in situ camera recording in Doublet Pool, for example, revealed that thumping occurs as bubbles collapse at the base of the pool as they exit the vent. The thumping might reflect the same process of eruption preparation for an active geyser (Vandemeulebrouck et al., 2013), but without sufficient energy transport, or needed conduit geometry, to initiate and sustain an eruption.

One of the central questions about unsteady hydrothermal systems is what controls variations during eruption or thumping cycles, which also directly addresses the question of eruption predictability. Investigating temporal variations of geyser eruptions has revealed connections between sequential eruption events, adjacent geysers, and changes triggered by seismic events (Eibl et al., 2021; Hurwitz et al., 2014; Husen et al., 2004; Hutchinson, 1985; Marler, 1964; Munoz-Saez, Namiki, et al., 2015; Munoz-Saez, Manga et al., 2015; Silver & Valette-Silver, 1992). While other environmental factors (e.g., air temperature, groundwater level, barometric pressure, wind speed) have also been proposed as potential factors that can influence the eruption cycle (Hurwitz et al., 2020, 2014; Marler, 1951; Reed et al., 2021), the physical processes that lead to the connections remain to be quantified. Laboratory and numerical geyser models have also been built to investigate how different factors might affect the eruption pattern (Adelstein et al., 2014; Ingebritsen & Rojstaczer, 1993, 1996; Namiki et al., 2016; Rudolph et al., 2018; Saptadji et al., 2016; Teshima et al., 2022). Systematically disentangling how each factor might affect the interval variation, and what these relationships mean for eruption processes, remains a subject to be understood (Hurwitz & Manga, 2017).

Here, we report the temporal variation of the Doublet Pool thumping cycle recorded by several geophone deployments across a 6 yr period. We use complementary measurements of environmental conditions to disentangle internal and external factors that affect the thumping cycle over hourly to multi-year time scales.

2. Data and Methods

Beginning in fall 2015, 3-component autonomous 5 Hz nodal geophones with a sampling rate of 1,000 Hz were deployed near Doublet Pool (Figure 1b) during seven campaigns (2015/11/2 to 2015/11/14, 2016/8/8 to 2016/8/12, 2016/11/7 to 2016/11/16, 2017/11/6 to 2017/11/18, 2018/9/30 to 2018/11/5, 2021/6/12 to 2021/7/14, and 2021/11/13 to 2021/11/17). The duration of each deployment varied and was constrained by either permitting, the battery capacity of the geophones (∼35 days), or weather. In November 2021, in addition to geophones, an Onset S-TMB-M002 temperature sensor was deployed in the main pool for ∼1.5 days. In April 2022, an In Situ Level Troll 500 pressure sensor was deployed to monitor changes in the water level of the pool for ∼4 days. Both in situ sensors collected data with a sampling rate of 1 Hz.

Strong hydrothermal tremor corresponding to active thumping periods can be observed in all the recorded seismograms (Figure 2a). We define the thumping interval as the time between each onset of thumping, and the silence interval (SI) as the time between the end of thumping to the onset of the next thumping period (Figure 2b). Despite the semi-regular thumping interval during each deployment, Doublet Pool clearly behaved differently across deployments; consistently shorter thumping intervals are observed in Fall 2018 compared to other times (Figure 2; Figure S1 in Supporting Information S1).

We adopt the STA/LTA (short-term-average over long-term-average amplitude ratio) technique (Allen, 1978) to automatically detect the active thumping cycle using the continuous seismic records. We calculate the vertical component root-mean-square amplitude using a 1.6 s running window for STA and an entire day for LTA. We empirically determine the STA/LTA ratio of 0.6 as the detection criterion for potential thumping signals, which

19448007, 2023, 4, Downloaded from https://agupubs.onlinelibrary.wiley.com/doi/10.1029/2022GL101175 by University Of Utah, Wiley Online Library on [15/02/2023]. See the Terms and Conditions (https://onlinelibrary.wiley.com/terms-and-conditions) on Wiley Online Library for rules of use; OA articles are governed by the applicable Creative Commons License

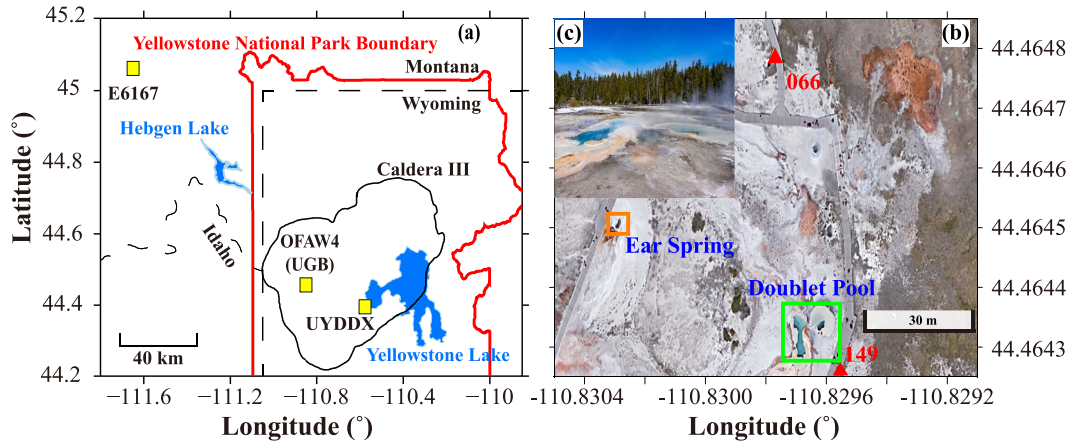

Figure 1. (a) Map of Yellowstone National Park (red curve) and the weather station locations (yellow squares). The dashed black lines show state boundaries, and the black solid curve outlines the 0.63 Ma Yellowstone caldera. The Upper Geyser Basin (UGB), where Doublet Pool is located, is ∼1.8 km northeast of weather station OFAW4. (b) Satellite image of the northern edge of Geyser Hill within the UGB showing seismic stations (red triangles) and the location of Ear Spring (orange box) and Doublet Pool (green box), which contains a main pool where thumping occurs (right) and an auxiliary pool (left). (c) Photo of Doublet Pool.

is mostly above the noise level but always below the thumping amplitude (Figure S2 in Supporting Information S1). To avoid including other undesired sporadic signals (e.g., earthquakes, anthropogenic noise, eruptions from nearby geysers), we only identify thumping when the STA/LTA ratio is continuously above 0.6 for at least 250 s. Using the beginning and ending time of each thumping time window, we determine the thumping duration, SI, and thumping interval (Figure 2b) for each thumping cycle. The results from stations 066 and 149 were highly consistent when both stations recorded synchronously. Besides 2015, in which only station 066 is available, we use data from station 149 for the following analyses.

To understand how the thumping cycle might be affected by external factors, we obtain wind speed, barometric pressure, and air temperature data from three nearby weather stations: OFAW4 (1.8 km away), UYDDX (21.6 km

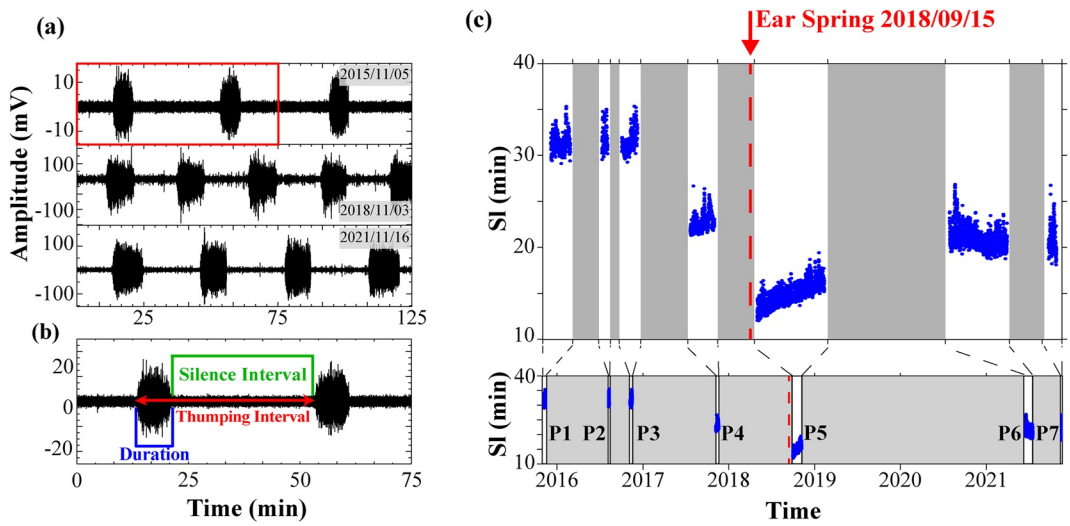

Figure 2. (a) Examples of recorded Doublet Pool seismic tremor for three different deployments. The red box identifies the zoomed-in waveform in (b). (b) Visualization of how the thumping duration, silence interval (SI), and thumping interval are defined in our study. (c) The observed SI variation (blue dots) throughout the entire experiment. The red dashed line indicates the date of the 2018 Ear Spring eruption. To better visualize the SI variations, the width of data windows (white) is exaggerated relative to data gaps (gray). The width of each data window is proportional to the number of days for each deployment, and the width of each data gap is proportional to the number of days without data. The lower panel shows the plot with an unperturbed time scale (P1–P7 mark the deployment periods).

19448007, 2023, 4, Downloaded from https://agupubs.onlinelibrary.wiley.com/doi/10.1029/2022GL101175 by University Of Utah, Wiley Online Library on [15/02/2023]. See the Terms and Conditions (https://onlinelibrary.wiley.com/terms-and-conditions) on Wiley Online Library for rules of use; OA articles are governed by the applicable Creative Commons License

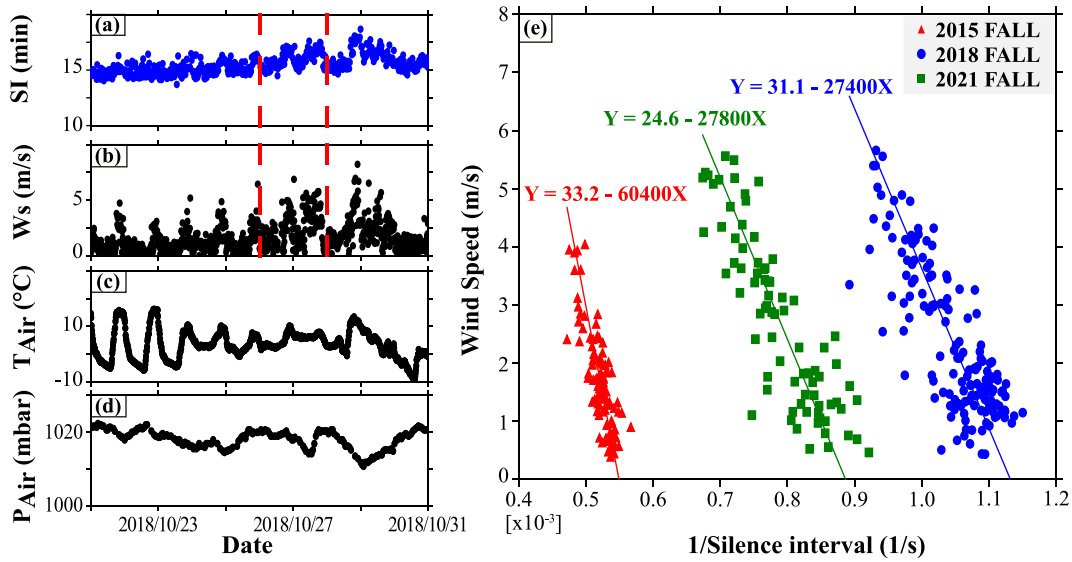

Figure 3. Example comparison between (a) SI, (b) wind speed, (c) air temperature, and (d) air pressure. The red dashed lines in (a and b) identify the 3-day window used in (e) for fall 2018. (e) The relationship between inverse SI and wind speed for 3-day example windows in 2015/11/12 to 2015/11/14 (red), 2018/10/26 to 2018/10/28 (blue), and 2021/11/16 to 2021/11/18 (green). The results of linear regressions are annotated.

away), and E6167 (93.2 km away) (Figure 1a). The data were downloaded from Mesowest (Mesowest, 2015). Station OFAW4 is closest to Doublet Pool, making it the best station to investigate the correlation between weather parameters and pool dynamics. We use station UYDDX only to fill in the data gap of OFAW4 in November 2017. As neither OFAW4 nor UYDDX provide barometric pressure data, we use the pressure record from station E6167 for the entire period.

3. Results and Discussion

The STA/LTA analysis identifies nearly 5,000 thumping cycles in our seismic records. We find that the thumping interval is mostly controlled by the SI (Figure S1 in Supporting Information S1), presumably representing the time needed to accumulate enough heat to initiate thumping. We thus focus on the implications of changes in the SI.

3.1. Variation of the Silence Interval

Figure 2c summarizes the seismically determined SI for each thumping cycle. Clear long-term variation is observed where the SI decreased from >30 min before 2016 to <15 min in 2018. A fast recovery is observed in the succeeding months and the SI seems to have stabilized above 20 min in 2021. To identify the mechanism(s) responsible for long-term variations in the SI, we assessed whether seismicity played a role since earthquakes can influence geysers (Husen et al., 2004; Manga & Brodsky, 2006). We observe no apparent relationship between the observed long-term SI variation and seismic events or deformation documented by GPS stations (Figures S3 and S4 in Supporting Information S1). The transition from decreasing to increasing SI in 2018 does coincide with an episode of changes to nearby thermal features on Geyser Hill, including the 15 September 2018 Ear Spring eruption (~60 m away, see Figure 1b). Prior to this eruption, the last major eruption at Ear Spring was in 1957. Following the 2018 eruption, boiling occurred in both of Doublet's pools and other nearby thermal features displayed altered activity (Kipple, 2018; Vaughan et al., 2020). The long-term Doublet Pool SI variation hence might reflect the heating and pressurization of the Geyser Hill system prior to 2018 which relaxed afterward.

On a several hour time scale, we observe smaller minute-scale SI changes (Figure 3a). To better understand the controlling factors, we compare the SI variation with wind speed, air temperature, and air pressure recorded by nearby weather stations (Figures 3b–3d). To quantify the comparison, we first segment all the time series into 3-day windows, with an overlap of 1 day between each window. For each 3-day window, we smooth the time

19448007, 2023, 4, Downloaded from https://agupubs.onlinelibrary.wiley.com/doi/10.1029/2022GL101175 by University Of Utah, Wiley Online Library on [15/02/2023]. See the Terms and Conditions (https://onlinelibrary.wiley.com/terms-and-conditions) on Wiley Online Library for rules of use; OA articles are governed by the applicable Creative Commons License

19448007, 2023, 4, Downloaded from https://agupubs.onlinelibrary.wiley.com/doi/10.1029/2022GL101175 by University Of Utah, Wiley Online Library on [15/02/2023]. See the Terms and Conditions (https://onlinelibrary.wiley.com/terms-and-conditions) on Wiley Online Library for rules of use; OA articles are governed by the applicable Creative Commons License

series by using a 30 min Gaussian running average and then calculate the correlation coefficients (CCs) between SI and each environmental factor. To account for potential timing errors and delays in response of the SI to weather factors, we search for the maximum CC in the time shift range between −120 and +120 min. Among all the environmental factors (Figures S5a–S5c in Supporting Information S1), the SI best correlated with wind speed with CC consistently higher than 0.5 when strong winds were present (Figures S5d and S5e in Supporting Information S1). This is consistent with an evaporative cooling model (Hurwitz et al., 2014) where strong winds accelerate heat removal from the pool and hence lengthen the SI (Hurwitz et al., 2008). A weaker correlation is also observed between SI and air temperature as stronger winds mostly occur during the daytime when the temperature is higher.

3.2. Energy Budget

The observed relationship between wind speed and SI allows us to estimate the excess heat influx H during the SI and the total energy U needed to initiate thumping. Following the energy budget analysis presented by Hurwitz et al. (2012), we set up the energy conservation equation:

$$U = \int_0^{\tau} H\,dt - \int_0^{\tau} AE\,dt \tag{1}$$

where A is the pool area (~54 m^2; Figure S6 in Supporting Information S1), E is the heat loss to the atmosphere per unit area, t is the time since the end of the previous thumping, τ is the SI (i.e., time needed to accumulate enough energy before thumping), and H is the difference between total heat influx H_{in} (i.e., base heating through convection, inflow) and outflux H_{out} (i.e., heat loss due to outflow) of the system, not including evaporative cooling. Assuming H and E are constant throughout the SI, the equation can be simplified as follows:

$$U = (H - AE)\tau. \tag{2}$$

When wind speed W_s and pool temperature are both high, following N. Fournier et al. (2009) and Hurwitz et al. (2012), the energy loss term E can be approximated as follows:

$$E \approx 8.1A^{-0.05}W_s e_s \tag{3}$$

where e_s represents the vapor pressure at the pool surface and all the variables are in standard units. For conciseness, Equation 3 retains only the dominant term. Substitution of heat loss (Equation 3) into the energy conservation Equation 2 leads to

$$W_s = \frac{H}{8.1A^{0.95}e_s} - \frac{U}{8.1A^{0.95}e_s} \cdot \frac{1}{\tau} \tag{4}$$

where wind speed W_s and inverse SI ($1/\tau$) are expected to be linearly related, consistent with our observations (Figure 3e).

For each 3-day window, we fit a line to the observed wind speed and inverse SI. Considering measurement errors in both the SI and wind speed, we determine the slope and intercept and their uncertainties (Deming, 1943). Only results from 3-day windows with CC > 0.5 between the wind speed and SI are considered reliable. In Fall 2021, with shallow pool temperature (~85°C averaged temperature during SI) measured by an in situ thermometer, we can estimate the vapor pressure e_s using the empirical relationship from equation A6 in N. Fournier et al. (2009). For the three 3-day windows with CC > 0.5, we calculate the mean and mean standard error of H and U to be 5.0 ± 0.2 MW (megawatt) and 5.7 ± 0.3 GJ (gigajoule), respectively. We note that the model treats the pool and connected deeper reservoirs as a single volume without capturing the details of recharge, discharge, and convection. Our goal, however, is to estimate a total energy budget.

Our estimated H represents the excess heat influx that deviates from the steady state and contributes to the energy accumulation during the SI. The excess heat U is lost during the active thumping period before the next SI. To assess the total heat influx H_{in}, heat outflux due to water outflow H_{out} should be accounted for. Using continuous pressure time series, we estimate a net volumetric refill rate of 2.2 ± 0.1 L/s based on the inferred water level change right after thumping (Figure S7 in Supporting Information S1). Based on mass balance, this corresponds

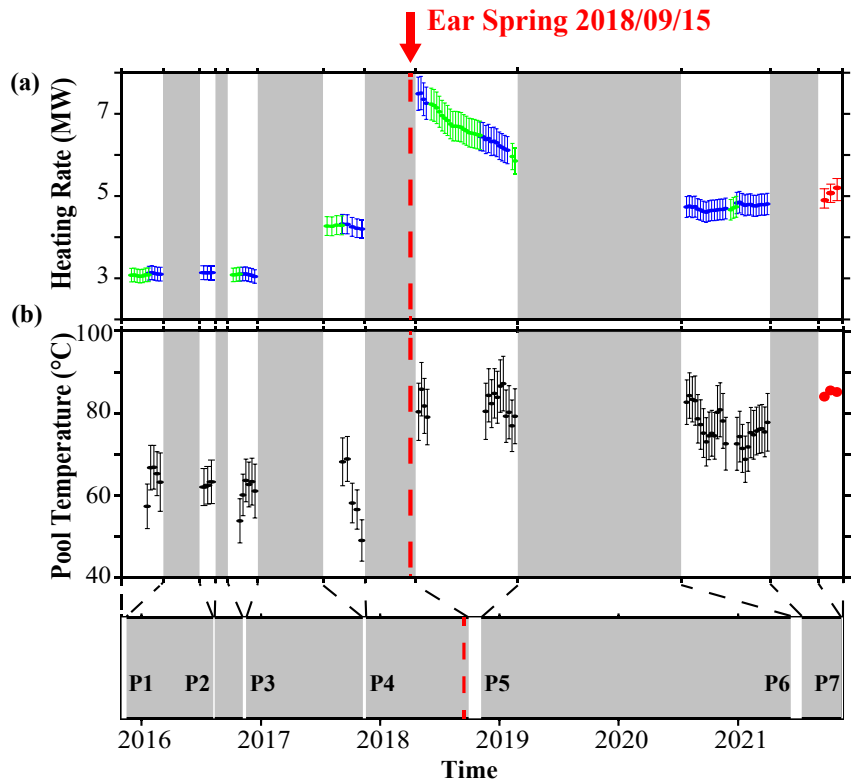

Figure 4. (a) The inferred basal heating rate of Doublet Pool. For each 3-day window, the estimated heating rate and its uncertainty are color-coded based on whether in situ pool temperature measurements are available (red) and if there is a high (>0.5; blue) or low (<0.5; green) CC between SI and the wind speed. The red dashed line shows the time of the Ear Spring eruption. The width of each data window is exaggerated relative to each gap window, similar to Figure 2c. (b) Similar to (a) but for surface pool temperature. Note that the pool temperature can only be estimated through the evaporative cooling model when there is a good correlation between SI and wind speed. The lower panel shows the unperturbed time scale.

to a ∼0.8 MW heat loss at the outflow channel when thermal water is released into the ambient environment (assuming an 85°C temperature difference). As this heat loss is about an order of magnitude smaller than H, we suggest the system keeps the majority of the base heat influx (minus the evaporative cooling) during SI (i.e., $H_{in} \approx H$).

The inferred energy discharge can be placed in perspective by comparison with other features and regional values. First, we consider other estimates in Yellowstone National Park. The total heat output is 12 MW for the Obsidian Pool Thermal Area and 8.8 MW for the Solfatara Plateau Thermal Area, where the advective heat output was ∼1.2 MW in both areas and dominated by conductive loss through the ground (Hurwitz et al., 2012). Favorito et al. (2021) report a mean heat output of 0.6 MW for 49 vents beneath Yellowstone Lake (factor of 10 1-sigma uncertainty, however). McMillan et al. (2018) estimated 85 MW for Excelsior Geyser. Karlstrom et al. (2013) measured 1.5 MW for Lone Star Geyser. From the chloride inventory method, the total thermal heat flow discharge from the Yellowstone hydrothermal system is 4–8 GW (R. O. Fournier, 1989; Hurwitz & Lowenstern, 2014). Moving outside of Yellowstone, Munoz-Saez et al. (2018) measured 0.14 MW for the very small El Jefe Geyser in El Tatio, Chile, and 121 MW for the entire basin. Thus, our inferred heat output has the same order of magnitude as that measured at other individual thermal features.

While we do not have temperature measurements outside fall 2021, if we assume heat U needed for thumping is the same, we can solve for the vapor pressure e_s (and hence the pool temperature) and the heat influx H for other time windows based on the result of the linear fitting (Figure 4). The estimated H, in general, follows the same trend of the SI where higher heat influx corresponds to shorter SI. This is expected as short-term SI changes due to wind are smaller than long-term SI changes related to heat influx. This may also explain the negative correlation between the thumping duration and SI (hence thumping interval; Figure S1a in Supporting

19448007, 2023, 4, Downloaded from https://agupubs.onlinelibrary.wiley.com/doi/10.1029/2022GL101175 by University Of Utah, Wiley Online Library on [15/02/2023]. See the Terms and Conditions (https://onlinelibrary.wiley.com/terms-and-conditions) on Wiley Online Library for rules of use; OA articles are governed by the applicable Creative Commons License

Information S1), as higher heat influx will not only make the system reach the threshold energy U faster but inject more heat into the system during thumping and hence prolong the thumping duration.

When ignoring the cooling due to wind, H is expected to be inversely related to the SI when assuming a constant U, as seen in Equation 2. Based on this observation, we also calculate H for time windows that did not pass the CC > 0.5 criterion presumably due to calm weather and hence the low wind speed variation. For these time windows, we estimated the SI with zero wind speed based on the lower 25th percentile of the SI distribution. H estimated either this way or based on the linear fitting is overall consistent (Figure 4a).

3.3. Implications for Hydrothermal Monitoring

The coincident changes at Doublet Pool and the eruption of Ear Spring suggest that there were broader-scale changes in the hydrothermal system in this part of the UGB. Changes in the SI and inferred heat input may reflect changes that would impact other hydrothermal features and could possibly lead to the formation of new features (Kipple, 2018; Vaughan et al., 2020). The shortening of the SI beginning in 2017 could thus be precursory to the eventual Ear Spring eruption and a sign of heating and pressurization of the Geyser Hill system. The lengthening of intervals since then would then be documenting a recovery. No obvious seismic event or deformation are connected to the inferred changes, suggesting that internal dynamics dominated changes in the hydrothermal system. Reed et al. (2021) drew a similar conclusion, that internal hydrothermal processes led to the reactivation of Earth's tallest active geyser, Steamboat, in 2018.

4. Conclusions

We monitored the hydrothermal thumping activity of Doublet Pool by deploying temporary seismic stations during seven campaigns, from 2015 to 2021. The silence interval (SI) at Doublet Pool varies over time scales from several hours to years. Variations on hourly time scales are dominated by evaporative cooling by wind, where strong winds enhance the removal of heat and vapor from the surface of the pool and hence lengthen the SI. Except for the 2018 Ear Spring eruption, its first major activity since 1957, no apparent connection can be established between seismic or deformation events and the SI over hourly to monthly time scales. A decrease of the SI between 2016 and 2018 and the subsequent recovery of the SI suggest that Doublet Pool might be responding to the heating and pressurization of a broader Geyser Hill system before 2018 that relaxed afterward. The reason for the reawakening of Ear Spring is still unknown but hints at possible connections between thermal features in the Geyser Hill area. We also quantified the energy budget of Doublet Pool based on energy conservation and estimated heat loss due to wind-driven evaporative cooling and water runoff. The estimated energy discharge is similar to other hydrothermal features in Yellowstone National Park and varies by a factor of more than two over the studied time period. From both short-term and long-term variations in the activity of Doublet Pool, we can separate surficial and deeper geothermal controls on activity. This study illustrates the value of continuous multi-parametric monitoring of active hydrothermal features which has the potential to disentangle internal and external factors that control the surficial manifestations of a hydrothermal system and could potentially warn of hazards such as hydrothermal explosions.

Data Availability Statement

The geophone data can be downloaded from an open repository (https://doi.org/10.5281/zenodo.7542427). The weather data can be downloaded from the Mesowest (https://mesowest.utah.edu/cgi-bin/droman/mesomap.cgi). The earthquake catalog around Yellowstone National Park can be downloaded from International Federation of Digital Seismograph Networks (FDSN; https://www.fdsn.org/networks/detail/WY/). The regional and teleseismic event catalog can be found on Geological Survey Comprehensive Earthquake Catalog (ComCat; https://earthquake.usgs.gov/earthquakes/map/). The GPS data can be downloaded from UNAVCO (https://www.unavco.org/instrumentation/networks/status/nota). The seismic data (University of Utah, 1983) can be downloaded from the Incorporated Research Institutions for Seismology (IRIS) Data Management Center (DMC) (https://ds.iris.edu/ds/nodes/dmc/forms/breqfast-request/).

19448007, 2023, 4, Downloaded from https://agupubs.onlinelibrary.wiley.com/doi/10.1029/2022GL101175 by University Of Utah, Wiley Online Library on [15/02/2023]. See the Terms and Conditions (https://onlinelibrary.wiley.com/terms-and-conditions) on Wiley Online Library for rules of use; OA articles are governed by the applicable Creative Commons License

Acknowledgments
This study is supported by the National Science Foundation 2116572 and 2116573. The authors thank Yellowstone National Park staff for supporting field deployments under Yellowstone research permits YELL-2015-SCI-0114, YELL-2016-SCI-0114, YELL-2017-SCI-0114, YELL-2018-SCI-8058, and YELL-2021-SCI-8058.

References

Adelstein, E., Tran, A., Saez, C. M., Shteinberg, A., & Manga, M. (2014). Geyser preplay and eruption in a laboratory model with a bubble trap. *Journal of Volcanology and Geothermal Research*, *285*, 129–135. https://doi.org/10.1016/j.jvolgeores.2014.08.005

Allen, R. V. (1978). Automatic earthquake recognition and timing from single traces. *Bulletin of the Seismological Society of America*, *68*(5), 1521–1532. https://doi.org/10.1785/BSSA0680051521

Bryan, T. S. (2008). *The geysers of Yellowstone* (4th ed.). University Press of Colorado.

Cannata, A., Di Grazia, G., Montalto, P., Ferrari, F., Nunnari, G., Patanè, D., & Privitera, E. (2010). New insights into banded tremor from the 2008–2009 Mount Etna eruption. *Journal of Geophysical Research: Solid Earth*, *115*(B12), B12318. https://doi.org/10.1029/2009JB007120

Deming, W. E. (1943). Statistical adjustment of data.

Eibl, E. P., Müller, D., Walter, T. R., Allahbakhshi, M., Jousset, P., Hersir, G. P., & Dahm, T. (2021). Eruptive cycle and bubble trap of Strokkur Geyser, Iceland. *Journal of Geophysical Research: Solid Earth*, *126*(4), e2020JB020769. https://doi.org/10.1029/2020JB020769

Favorito, J. E., Harris, R. N., Sohn, R. A., Hurwitz, S., & Luttrell, K. M. (2021). Heat flux from a vapor-dominated hydrothermal field beneath Yellowstone Lake. *Journal of Geophysical Research: Solid Earth*, *126*(5), e2020JB021098. https://doi.org/10.1029/2020JB021098

Fournier, N., Witham, F., Moreau-Fournier, M., & Bardou, L. (2009). Boiling Lake of Dominica, West Indies: High-temperature volcanic Crater Lake dynamics. *Journal of Geophysical Research: Solid Earth*, *114*(B2), B02203. https://doi.org/10.1029/2008JB005773

Fournier, R. O. (1989). Geochemistry and dynamics of the Yellowstone National Park hydrothermal system. *Annual Review of Earth and Planetary Sciences*, *17*(1), 13–53. https://doi.org/10.1146/annurev.ea.17.050189.000305

Fujita, E. (2008). Banded tremor at Miyakejima volcano, Japan: Implication for two-phase flow instability. *Journal of Geophysical Research: Solid Earth*, *113*(B4), B04207. https://doi.org/10.1029/2006JB004829

Hurwitz, S., Harris, R. N., Werner, C. A., & Murphy, F. (2012). Heat flow in vapor dominated areas of the Yellowstone Plateau Volcanic Field: Implications for the thermal budget of the Yellowstone Caldera. *Journal of Geophysical Research: Solid Earth*, *117*(B10). https://doi.org/10.1029/2012JB009463

Hurwitz, S., King, J. C., Pederson, G. T., Martin, J. T., Damby, D. E., Manga, M., et al. (2020). Yellowstone's Old Faithful Geyser shut down by a severe 13th century drought. *Geophysical Research Letters*, *47*(20), e2020GL089871. https://doi.org/10.1029/2020GL089871

Hurwitz, S., Kumar, A., Taylor, R., & Heasler, H. (2008). Climate-induced variations of geyser periodicity in Yellowstone National Park, USA. *Geology*, *36*(6), 451–454. https://doi.org/10.1130/G24723A.1

Hurwitz, S., & Lowenstern, J. B. (2014). Dynamics of the Yellowstone hydrothermal system. *Reviews of Geophysics*, *52*(3), 375–411. https://doi.org/10.1002/2014RG000452

Hurwitz, S., & Manga, M. (2017). The fascinating and complex dynamics of geyser eruptions. *Annual Review of Earth and Planetary Sciences*, *45*(1), 31–59. https://doi.org/10.1146/annurev-earth-063016-015605

Hurwitz, S., Sohn, R. A., Luttrell, K., & Manga, M. (2014). Triggering and modulation of geyser eruptions in Yellowstone National Park by earthquakes, Earth tides, and weather. *Journal of Geophysical Research: Solid Earth*, *119*(3), 1718–1737. https://doi.org/10.1002/2013JB010803

Husen, S., Taylor, R., Smith, R. B., & Healser, H. (2004). Changes in geyser eruption behavior and remotely triggered seismicity in Yellowstone National Park produced by the 2002 M 7.9 Denali fault earthquake, Alaska. *Geology*, *32*(6), 537–540. https://doi.org/10.1130/G20381.1

Hutchinson, R. A. (1985). Hydrothermal changes in the Upper Geyser Basin, Yellowstone National Park, after the 1983 Borah Peak, Idaho, earthquake. In *Proceedings of Workshop* (Vol. 28, pp. 612–624).

Ingebritsen, S. E., & Rojstaczer, S. A. (1993). Controls on geyser periodicity. *Science*, *262*(5135), 889–892. https://doi.org/10.1126/science.262.5135.889

Ingebritsen, S. E., & Rojstaczer, S. A. (1996). Geyser periodicity and the response of geysers to deformation. *Journal of Geophysical Research: Solid Earth*, *101*(B10), 21891–21905. https://doi.org/10.1029/96JB02285

Karlstrom, L., Hurwitz, S., Sohn, R., Vandemeulebrouck, J., Murphy, F., Rudolph, M. L., et al. (2013). Eruptions at Lone Star Geyser, Yellowstone National Park, USA: 1. Energetics and eruption dynamics. *Journal of Geophysical Research: Solid Earth*, *118*(8), 4048–4062. https://doi.org/10.1002/jgrb.50251

Kedar, S., Kanamori, H., & Sturtevant, B. (1998). Bubble collapse as the source of tremor at Old Faithful Geyser. *Journal of Geophysical Research: Solid Earth*, *103*(B10), 24283–24299. https://doi.org/10.1029/98JB01824

Kedar, S., Sturtevant, B., & Kanamori, H. (1996). The origin of harmonic tremor at Old Faithful Geyser. *Nature*, *379*(6567), 708–711. https://doi.org/10.1038/379708a0

Kipple, M. (2018). The north Geyser Hill disturbance, September 2018. *The Geyser Gazer Sput*, *32*(5), 6–12.

Legaz, A., Revil, A., Roux, P., Vandemeulebrouck, J., Gouedard, P., Hurst, T., & Bolève, A. (2009). Self-potential and passive seismic monitoring of hydrothermal activity: A case study at Iodine Pool, Waimangu geothermal valley, New Zealand. *Journal of Volcanology and Geothermal Research*, *179*(1–2), 11–18. https://doi.org/10.1016/j.jvolgeores.2008.09.015

Manga, M., & Brodsky, E. (2006). Seismic triggering of eruptions in the far field: Volcanoes and geysers. *Annual Review of Earth and Planetary Sciences*, *34*(1), 263–291. https://doi.org/10.1146/annurev.earth.34.031405.125125

Marler, G. D. (1951). Exchange of function as a cause of geyser irregularity (Wyoming). *American Journal of Science*, *249*(5), 329–342. https://doi.org/10.2475/ajs.249.5.329

Marler, G. D. (1964). *Effects of the Hebgen Lake earthquake of 17 August 1959, on the hot springs of the Firehole Geyser basins, Yellowstone National Park*. U.S. Government Printing Office.

McMillan, N., Larson, P., Fairley, J., Mulvaney-Norris, J., & Lindsey, C. (2018). Direct measurement of advective heat flux from several Yellowstone hot springs, Wyoming, USA. *Geosphere*, *14*(4), 1860–1874. https://doi.org/10.1130/GES01598.1

Mesowest. (2015). University of Utah. Retrieved from http://mesowest.utah.edu/

Munoz-Saez, C., Manga, M., & Hurwitz, S. (2018). Hydrothermal discharge from the El Tatio basin, Atacama, Chile. *Journal of Volcanology and Geothermal Research*, *361*, 25–35. https://doi.org/10.1016/j.jvolgeores.2018.07.007

Munoz-Saez, C., Manga, M., Hurwitz, S., Rudolph, M. L., Namiki, A., & Wang, C. Y. (2015). Dynamics within geyser conduits, and sensitivity to environmental perturbations: Insights from a periodic geyser in the El Tatio Geyser field, Atacama Desert, Chile. *Journal of Volcanology and Geothermal Research*, *292*, 41–55. https://doi.org/10.1016/j.jvolgeores.2015.01.002

Munoz-Saez, C., Namiki, A., & Manga, M. (2015). Geyser eruption intervals and interactions: Examples from El Tatio, Atacama, Chile. *Journal of Geophysical Research: Solid Earth*, *120*(11), 7490–7507. https://doi.org/10.1002/2015JB012364

Namiki, A., Ueno, Y., Hurwitz, S., Manga, M., Munoz-Saez, C., & Murphy, F. (2016). An experimental study of the role of subsurface plumbing on geothermal discharge. *Geochemistry, Geophysics, Geosystems*, *17*(9), 3691–3716. https://doi.org/10.1002/2016GC006472

Nayak, A., Manga, M., Hurwitz, S., Namiki, A., & Dawson, P. B. (2020). Origin and properties of hydrothermal tremor at Lone Star Geyser, Yellowstone National Park, USA. *Journal of Geophysical Research: Solid Earth*, *125*(12), e2020JB019711. https://doi.org/10.1029/2020JB019711

19448007, 2023, 4, Downloaded from https://agupubs.onlinelibrary.wiley.com/doi/10.1029/2022GL101175 by University Of Utah, Wiley Online Library on [15/02/2023]. See the Terms and Conditions (https://onlinelibrary.wiley.com/terms-and-conditions) on Wiley Online Library for rules of use; OA articles are governed by the applicable Creative Commons License

Reed, M. H., Munoz-Saez, C., Hajimirza, S., Wu, S. M., Barth, A., Girona, T., et al. (2021). The 2018 reawakening and eruption dynamics of Steamboat Geyser, the world's tallest active geyser. *Proceedings of the National Academy of Sciences*, *118*(2), e2020943118. https://doi.org/10.1073/pnas.2020943118

Rinehart, J. S. (1980). *Geysers and geothermal energy* (Vol. 223). Springer-Verlag. https://doi.org/10.1007/978-1-4612-6084-4

Rudolph, M. L., Sohn, R. A., & Lev, E. (2018). Fluid oscillations in a laboratory geyser with a bubble trap. *Journal of Volcanology and Geothermal Research*, *368*, 100–110. https://doi.org/10.1016/j.jvolgeores.2018.11.003

Saptadji, N., O'Sullivan, J., Krzyzosiak, W., & O'Sullivan, M. (2016). Numerical modeling of Pohutu Geyser, Rotorua, New Zealand. *Geothermics*, *64*, 401–409. https://doi.org/10.1016/j.geothermics.2016.06.019

Silver, P. G., & Valette-Silver, N. J. (1992). Detection of hydrothermal precursors to large Northern California earthquakes. *Science*, *257*(5075), 1363–1368. https://doi.org/10.1126/science.257.5075.1363

Smith, R. B., & Siegel, L. J. (2000). *Windows into the Earth: The geologic story of Yellowstone and Grand Teton National Parks*. Oxford University Press.

Teshima, N., Toramaru, A., & Ichihara, M. (2022). Precursory pressure oscillation in a laboratory geyser system. *Journal of Volcanology and Geothermal Research*, *429*, 107613. https://doi.org/10.1016/j.jvolgeores.2022.107613

Toramaru, A., & Maeda, K. (2013). Mass and style of eruptions in experimental geysers. *Journal of Volcanology and Geothermal Research*, *257*, 227–239. https://doi.org/10.1016/j.jvolgeores.2013.03.018

University of Utah. (1983). Yellowstone National Park Seismograph Network [Dataset]. International Federation of Digital Seismograph Networks. https://doi.org/10.7914/SN/WY

Vandemeulebrouck, J., Roux, P., & Cros, E. (2013). The plumbing of Old Faithful Geyser revealed by hydrothermal tremor. *Geophysical Research Letters*, *40*(10), 1989–1993. https://doi.org/10.1002/grl.50422

Vandemeulebrouck, J., Sohn, R. A., Rudolph, M. L., Hurwitz, S., Manga, M., Johnston, M. J., et al. (2014). Eruptions at Lone Star Geyser, Yellowstone National Park, USA: 2. Constraints on subsurface dynamics. *Journal of Geophysical Research: Solid Earth*, *119*(12), 8688–8707. https://doi.org/10.1002/2014JB011526

Vaughan, R. G., Hungerford, J. D., & Keller, W. (2020). A newly emerging thermal area in Yellowstone. *Frontiers of Earth Science*, *8*, 204. https://doi.org/10.3389/feart.2020.00204

White, D. E. (1967). Some principles of geyser activity, mainly from Steamboat Springs, Nevada. *American Journal of Science*, *265*(8), 641–684. https://doi.org/10.2475/ajs.265.8.641

Wu, S. M., Lin, F. C., Farrell, J., & Allam, A. (2019). Imaging the deep subsurface plumbing of Old Faithful Geyser from low-frequency hydrothermal tremor migration. *Geophysical Research Letters*, *46*(13), 7315–7322. https://doi.org/10.1029/2018GL081771

Wu, S. M., Lin, F. C., Farrell, J., Keller, W. E., White, E. B., & Hungerford, J. D. (2021). Imaging the subsurface plumbing complex of Steamboat Geyser and Cistern Spring with hydrothermal tremor migration using seismic interferometry. *Journal of Geophysical Research: Solid Earth*, *126*(4), e2020JB021128. https://doi.org/10.1029/2020JB021128

Wu, S. M., Ward, K. M., Farrell, J., Lin, F. C., Karplus, M., & Smith, R. B. (2017). Anatomy of Old Faithful from subsurface seismic imaging of the Yellowstone Upper Geyser Basin. *Geophysical Research Letters*, *44*(20), 10–240. https://doi.org/10.1002/2017GL075255

References From the Supporting Information

Wang, C. Y., & Chia, Y. (2008). Mechanism of water level changes during earthquakes: Near field versus intermediate field. *Geophysical Research Letters*, *35*(12). https://doi.org/10.1029/2008GL034227

19448007, 2023, 4, Downloaded from https://agupubs.onlinelibrary.wiley.com/doi/10.1029/2022GL101175 by University Of Utah, Wiley Online Library on [15/02/2023]. See the Terms and Conditions (https://onlinelibrary.wiley.com/terms-and-conditions) on Wiley Online Library for rules of use; OA articles are governed by the applicable Creative Commons License